

# Evaluating the Nonlinear Dynamic Stiffness of Rail Pad using Finite Element Method

Mohamad Hazman Halim, Abdul Malek Abdul Wahab\*,  
Muhamad Sukri Hadi

School of Mechanical Engineering, College of Engineering,  
Universiti Teknologi MARA, 40450 Shah Alam, Selangor, MALAYSIA  
\*abdmalek@uitm.edu.my

Azmi Ibrahim

School of Civil Engineering, College of Engineering,  
Universiti Teknologi MARA, 40450 Shah Alam, Selangor, Malaysia

Noraishah Mohamad Noor

Rapid Rail Sdn. Bhd, Kuala Lumpur, MALAYSIA

## ABSTRACT

*Unwanted vibration and noise from railroads have a significant negative impact on the environment, causing damage to roads, buildings, and other structures. To mitigate this condition, rail pads have been installed as dampers to lessen the impact of vibration and shock on the railway track. The rail pad is made of a polymeric substance having nonlinear properties. This research examined the dynamic stiffness of rail pads made of thermoplastic elastomers (TPEs). ANSYS software was used to estimate the impact of temperature, toe load, and frequency under dynamic loading. The three-dimensional (3D) finite element model (FE) was created based on hyperelastic theory. The dynamic stiffness of the interlayer decreases with increasing temperature. For the effect of peak load and frequency, both parameters were directly proportional to dynamic stiffness. An increase in either parameter results in a stiffening of the interlayer. Frequency has the least effect on the dynamic stiffness of the track bed compared to temperature and peak load, with the average percentage difference between high and low being 28.31%, 55.57%, and 21.9%, respectively.*

**Keywords:** *Rail Pad; Dynamic Load; Deformation; Temperature; Frequency*

## Introduction

An important part of the railroads that keeps the operation running smoothly is the rail fastening system [1]. The rail pad, which is positioned below the rail, is one of the crucial parts of the fastening mechanism [2]–[4]. The rail pad's primary purpose is to provide sufficient vertical rigidity for ballasted and slab track [5]–[6]. Elastic rail pads are a practical way to lessen wheel/rail contact, slow down ballast pulverization, and minimize railroad maintenance expenses. The sleeper's protection is one of the rail pad's purposes [7]–[8]. Additionally, the rail pad enhances the ballast's protection from larger dynamic overloads [9]–[10].

The materials used to create the rail pads have significant nonlinear and dissipative mechanical properties that are greatly impacted by the loads and environmental conditions [11]. The excitation frequency [12]–[13], the amplitude of the load [14]–[15], the temperature [16], and the rail pad stiffness [13], [17] are all factors that have been documented in previous research.

The mechanical properties of rail pads in operation settings have been examined through several experimental investigations and numerical calculations. Fenander [12] investigated the reaction of the pads using experimental work and discovered that stiffness very slightly increases with frequency and dramatically rises with preload. To improve the accuracy of the forecast of the broadband vibration and noise produced by high-speed rail vehicles, experimental research was undertaken to acquire frequency-dependent dynamic performance of high-speed rail pads during the passage of rail cars [13]. The experimental work by Kaewunruen et al. [7] stated that the track surface (or vertical deviation) tends to deform at larger displacement amplitude and resonates at a lower wavelength of track roughness under dynamic conditions.

Wei et al. [14] modelled the rail pad numerically using the finite element method (FEM) and found that the vertical stiffness of TPE rail pads changed with load amplitude. Koroma et al. stated that it was important to consider the preload effect on predicting the dynamic stiffness of TPEs rail pads using FE analysis [18]. To explore the effects of the stimulation frequency and displacement amplitude, Zhu et al. [15] modelled the rail pad using 3D-CVST.

Analysing the rail pad geometry solutions in terms of deformation will consume a long time to complete the result by having the experimental approach in the laboratory. In earlier investigations, a variety of numerical calculation methods for estimating the dynamic stiffness of rail pads were investigated. Unfortunately, there needs to be more development

in analysing the rail pad hyperelastic material dynamic stiffness using finite element (FE) modelling. Therefore, this work predicted the behaviour of dynamic stiffness for a particular rail pad material, thermoplastic elastomers (TPEs), using FE analysis. The 3D model was established using ANSYS software. On dynamic stiffness, the effects of temperature, toe stress, and frequency were anticipated.

The laboratory and field investigation could have been more extensive in budget and time for design options. As a result, the FE method was created to analyse the impact of key factors quickly. The proposed model may be used to evaluate how rail pads' dynamic stiffness would behave under various parametric circumstances. FE analysis can be employed as a decision-support tool for maintenance practitioners to evaluate the dynamic stiffness of railpads. This enables them to make well-informed decisions about maintenance strategies. By using FE analysis, practitioners can identify areas that require improvement, predict the performance of various railpad configurations, and optimize maintenance interventions. These actions aim to enhance overall track performance and minimize long-term costs.

## **Material and Method**

### **Rail pad**

The material of the rail pad in this study is thermoplastic elastomers (TPEs). The rail pad is a rubber-like material that exhibits nonlinear behaviour. The hyperelastic model is used to show the nonlinear behaviour of the rail pad for rubber-like materials. Equation (1) shows the general principal stresses for the Ogden model. As shown in Equation (2), the Ogden formula was applied to model the dynamic stiffness characteristic of rail pads under uniaxial dynamic load [19]. The rail pad's dimensions are 150 mm long, 150 mm wide, and 8 mm thick ( $l \times w \times t$ ).

The Ogden model is an all-encompassing hyperelasticity model with a Helmholtz free energy per reference volume stated in terms of the major stretches being used. There are numerous ways to express the Ogden model's Helmholtz free energy. The principal stresses  $\sigma_i$ ,  $i \in [1]-[3]$ , for the Ogden model, are given by:

$$\sigma_i = \frac{2}{J} \sum_{k=1}^N \frac{\mu_k}{\alpha_k} ((\lambda^*_i)^{\alpha_k} - \frac{1}{3} [(\lambda^*_1)^{\alpha_k} + (\lambda^*_2)^{\alpha_k} + (\lambda^*_3)^{\alpha_k}]) + \sum_{k=1}^N \frac{2k}{D_k} (J - 1)^{2k-1} \quad (1)$$

where  $J$  is a Jacobian determinant,  $N$  is the number of chains per reference unit volume,  $\alpha$  is the shear displacement, and  $\mu$  is the shear modulus. The indices  $i$  and  $j$  take the values 1, 2, and 3. Then, the stresses from the incompressible Ogden model in uniaxial loading are given by;

$$\sigma_{uniax} = \frac{2}{J} \sum_{k=1}^N \frac{2\mu_k}{\alpha_k} \left[ \lambda^{\alpha_k} - \left( \frac{1}{\sqrt{\lambda}} \right)^{\alpha_k} \right] \quad (2)$$

### Rail and sleeper

To represent the rail and sleeper, a solid element with a nominal cross-sectional form was employed. Steel and concrete were used to make the rail and sleeper, respectively. In solid materials like steel and concrete, linear elasticity is a normal technique for modelling the mechanical behaviour of very small strains [20]-[21]. The rail constructions' characteristics and attenuation factors are stated in Othman et al. [22]. The figures were gathered from various scientific journals and the web's typical material attributes.

### Simulation test campaign

CATIA V5 software was used to generate the models for the rail, rail pad, and sleeper. The International Union of Railways (UIC) design guidelines were followed when creating the steel rail. Figure 1 depicts in isometric detail the rail, rail pad, and sleeper in 3D.

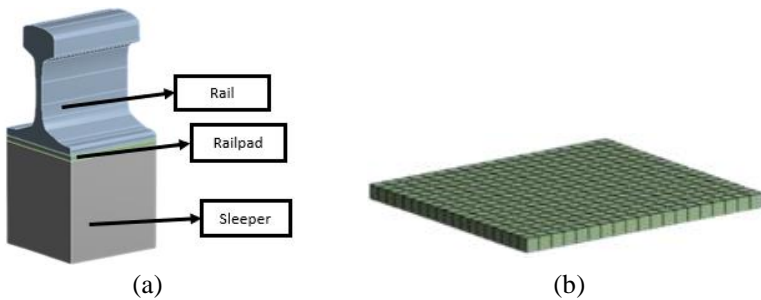


Figure 1: 3D Model of (a) simplified fastening system, and (b) rail pad [22]

The fastening system's 3D model was then imported into the ANSYS programme for analysis as well as simulation. It was projected that toe load, temperature, and frequency would have an impact on the TPE's dynamic stiffness. Standard toe load measurements are 18 kN. The toe load occurred in three instances. First, the scenario that reflected the 18 kN system's appropriate assembly. Then, 5 kN and 30 kN of under- or over-torque,

respectively, were studied. These were assessed to demonstrate the impact of excessive toe load tightness.

Starting at the typical room temperature of 20 °C, the simulation was run at various temperatures. Considering Malaysian conditions, a 52 °C maximum and a 0 °C minimum temperature were used for the test. The hottest temperature ever recorded in Malaysia was 40.1 °C. However, the rail pad's temperature might reach as high as 52 °C due to heating brought on by the wheels' repetitive motion over the railway. To use comparable temperature ranges, four distinct temperatures were included (0 °C, 20 °C, 35 °C, and 52 °C).

### **Boundary conditions and meshing**

Figure 2 demonstrates the finite element method's applied toe load, load, and boundary conditions, incorporating frictionless and fixed support. The force produced as wheels pull on rails is known as the applied load. The load was time-based in cycles and for each steadily raised load applied, the deformation of the rail pad was recorded. An imposed boundary condition is used in this simulation. It was used at the base of the concrete sleeper as a fixed support. On the edges of the rail pad, frictionless support was used. While the simulation analysis is being performed, these boundary conditions give mediocre support and prohibit any component from moving freely.

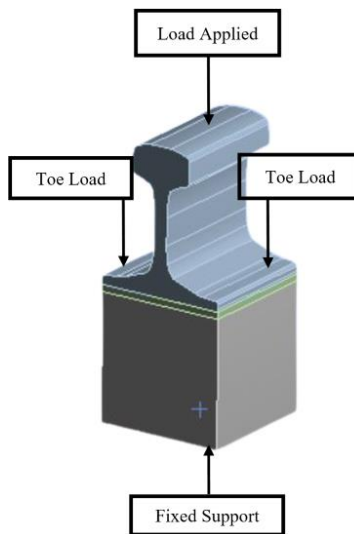


Figure 2: Boundary condition for fastening system railway track [22]

The contact between two surfaces also impacts the simulation results. The location of the interaction was therefore established. A friction

coefficient was used to identify the rail, sleeper, and rail pad as having frictional contact. In this work, the friction coefficient was set at 0.16 [23]. Two distinct geometries in this frictional contact can convey shear stresses. That kind of circumstance is referred to as “sticking”.

Mesh creation is necessary for any physical problem's finite element model. Nodes and elements are used to define it. The 3D element was used to model the fastening system. All components (rail, concrete, and rail pad) used the multi-zone method for meshing. This meshing technique was frequently employed due to speed and accuracy. The multi-zone approach is the best meshing technique since it discretized the model with the fewest number of elements while simultaneously having the highest element quality and least skewness [24]. One advantage of the multi-zone approach in this context is the ability to tailor the mesh resolution to different regions of the rail pad, ensuring higher accuracy where it is most needed. This adaptability is particularly beneficial in capturing the complex behaviour of rail pads, which experience nonlinear effects due to their material properties and the dynamic loads imposed on them. The element quality and skewness of the mesh were assessed to guarantee a high mesh grade.

### Dynamic analysis

Elastic deformation,  $\delta$  is required to determine the rail pad's dynamic stiffness. The following equations can be used to compute this:

$$\delta = \frac{\sigma \times L}{E} = \frac{F \times L}{A \times E} \quad (3)$$

where the normal stress  $\sigma$ , the elastic modulus  $E$ , the force  $F$ , the length  $L$ , and the area  $A$  are present, for computing the modulus of elasticity  $E$ , the equation is:

$$E = \frac{\sigma}{\varepsilon} \quad (4)$$

where  $\varepsilon$  represents the strain. This can be determining the average stress  $\sigma$ , using the formula below:

$$\sigma = \frac{P}{A} \quad (5)$$

where  $A$  is the area and  $P$  is the normal force.

Dynamic tests were used to assess the effects of different service conditions on the pad. Thus, in this work, the dynamic stiffness under the influence of different temperatures, toe loads, and frequency were estimated.

The dynamic testing utilised the three amplitudes described in standards EN 13481-2 and EN-13146-9 [25].

TPE rail pad material was used for the test in the dynamic simulation, and it was exposed to reference conditions such as the applied load, toe load, and boundary condition. For dynamic analysis, the finite element equations of motion were numerically time-integrated [25]. The rail pad in Figure 3 underwent a dynamic examination by having 100 sinusoidal cycles for each load applied. The deformation of the rail pad for each load was recorded.

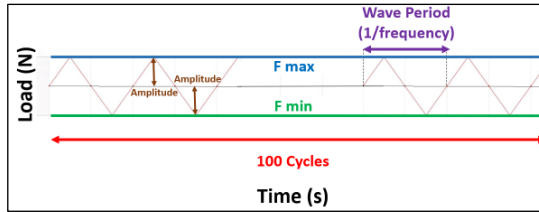


Figure 3: Dynamic cycle of load-deformation

## Results and Discussion

### Validation

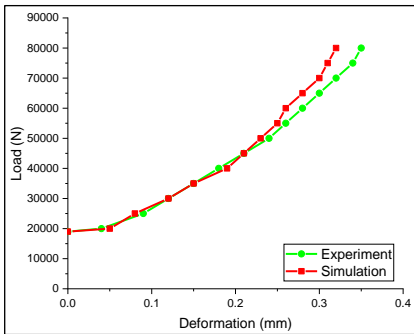
For validation of the simulation model, a mesh convergence test was performed. The parameters for the mesh setup considered in this investigation are shown in Table 1. The deformation of rail for load 80 kN starts stabilized at 10 mm size of elements. The simulations with sizes of elements 10 mm, 9 mm, and 8 mm produced readings comparable to those in the validation research study [25]. However, it took longer than the simulation to complete as the size of the element decreased. As the size of elements reduces, the number of nodes and elements increases. This contributes to the longer time taken for the simulation to complete. Therefore, 10 mm was used for further simulation in the current investigation, as the time taken for completion was less compared smaller size of elements.

Figures 4(a) and 4(b) demonstrate the outcomes for load displacement in dynamic analysis. The load was applied at 5 kHz for 100 cycles. The toe load was 18 kN and the temperature was at 20 °C, known as the reference condition. This numerical computation followed the experimental setting of the previous study [25]. For the results, the average value of 100 cycles of deformation was taken. The dynamic compressive force that nonlinearly boosted the rail pad's displacement is seen in Figure 4(a). Figure 4(b) shows displacement is high at the edge of the railpad at a maximum load of 80 kN. These dynamic loads can lead to stress redistribution within the railpad

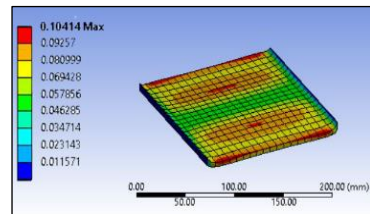
material, causing higher displacement at the edge where the load is concentrated. The simulation's results agree with those reported by Sainz-Aja et al.'s experimental test [25]. The average percentage error was 4.68%, as tabulated in Table 2. The rigid body displacement, which occurred at 20 kN, 30 kN, and 40 kN, was corrected for accurate results. This was a common problem for geometrically nonlinear small-strain conditions [26]. As a percentage error below 10%, it was concluded that the simulation model could be accepted.

Table 1: Mesh convergence analysis

Size of element (mm)	Nodes	Elements	Time consumption (min)	Average total deformation at 80 kN (mm)
19.4	28457	5624	24	0.40
16.0	32505	6555	27	0.39
12.0	37267	7650	30	0.38
10.0	39648	8197	30	0.33
9	40838	8470	32	0.33
8	42028	8743	33	0.33



(a)



(b)

Figure 4: (a) Evaluating the contrasts between simulation versus experiment results [25], and (b) TPE rail pad displacement

## Dynamic stiffness assessment

### The influence of temperature

Throughout the operation, the rail pad is exposed to a range of temperatures. Figure 5 demonstrates how temperature affects the TPE rail pad's dynamic stiffness. The temperature that has been analysed were 0 °C, 20 °C, 35 °C, and 52 °C. The load was applied at 5 kHz for 100 cycles. 18 kN was the toe

load for both sides and the applied load was up to 80,000 kN in the step of 5000 kN. The deformation of rail pad increase as temperature increase. This trend is in agreement with previous work [27]-[28]

Table 2: Comparing simulation and experimental results [25]

Load (N)	Deformation		Percentage error (%)
	Reference	Simulation	
19000	0.00	0.00	0.00
20000	0.04	0.05	11.43
25000	0.09	0.08	6.90
30000	0.12	0.12	1.47
35000	0.15	0.15	0.52
40000	0.18	0.19	3.03
45000	0.21	0.21	0.68
50000	0.24	0.23	4.97
55000	0.26	0.25	6.91
60000	0.28	0.26	6.23
65000	0.30	0.28	6.64
70000	0.32	0.30	5.83
75000	0.34	0.31	6.43
80000	0.35	0.33	5.71

Figure 6 illustrates the effect of temperature on the elongation of a railpad under a maximum load of 80 kN. The red colour area is the highest deformation while the blue colour area shows the lowest deformation occurs. At a temperature of 0 °C, the highest deformation value is 0.0821 mm at the near centre of railpad. As the temperature increases, the highest deformation moves towards the edge of railpad. For temperature 52 °C, the highest deformation is 0.1697 mm more than 51% increment. At the highest temperature, the areas experiencing significant elongation were predominantly located at the edges of the railpad, as compared to the lowest temperature in this study. The value of maximum deformation increases as the temperature increases.

Table 3 shows the percentage difference of deformation between the lowest and highest temperatures at 0 °C and 52 °C, respectively. The average percentage difference between 0 °C and 52 °C is 28.31% for the stated dynamic load applied. The deformation difference decreases as the dynamic load increases. At 2 kN load, the percentage difference of deformation is 63.98%. As the load reaches 80 kN, the percentage difference of deformation reduces to 11.91%. This demonstrates how the impact of temperature diminishes as dynamic load increases.

Reduced dynamic stiffness is a result of increased rail pad displacement. Thus, increasing temperature leads to a lessening in dynamic

stiffness [25]. The rail pads' elastic modulus will decrease as the temperature rises. As a result, the rail pads endure greater deformation the lower their modulus of elasticity. In general, the temperature has an inverse relationship with the rail pad's stiffness. As a result, the rail pad's rigidity declines as the temperature rises. Temperature increases molecular mobility, thereby allowing the rail pads to lengthen at a microscopic level. However, as the compression load increases, the molecular mobility is restricted, resulting in less deformation due to temperature. According to the underlying theory of materials science, the inverse relationship between temperature and rail pad stiffness can be explained by increased molecular mobility at higher temperatures, leading to greater microscopic lengthening of the rail pad, while increased compression load restricts molecular mobility, resulting in reduced deformation due to temperature.

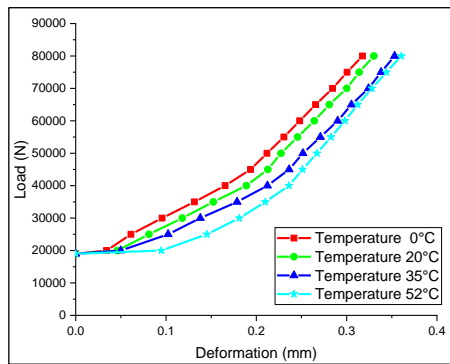


Figure 5: The rail pad deformation for different temperature

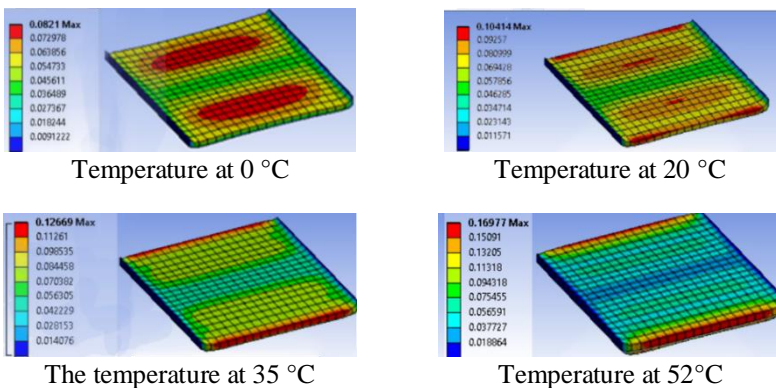


Figure 6: The effect of temperature on the elongation of rail pads at a maximum load of 80 kN

Table 3: Comparison of deformation differences between high and low temperatures for different loads.

Load (N)	Deformation		Differences (%)
	0 °C	52 °C	
19000	0.00	0.00	0
20000	0.03	0.09	63.98
25000	0.06	0.15	57.87
30000	0.10	0.18	47.20
35000	0.13	0.21	37.39
40000	0.17	0.24	29.94
45000	0.19	0.25	22.90
50000	0.21	0.27	20.73
55000	0.23	0.28	18.45
60000	0.25	0.30	16.80
65000	0.27	0.31	14.94
70000	0.28	0.33	13.30
75000	0.30	0.34	12.65
80000	0.32	0.36	11.91

**Effect of toe load**

Figure 7 shows the impact of various toe loads, 5 kN, 18 kN, and 30 kN, the TPE rail pad's dynamic stiffness under reference conditions (at a temperature 20 °C). Increasing the toe load results in an increase in the vertical dynamic stiffness. The highest railpad deformation occurred at toe load 30 kN rather than 5 kN and 18 kN. The significance of the gap difference also shows the difference between 5 kN and 30 kN compared to 18 kN and 30 kN in its deformation value. The results agreed with previous work carried out by Sainz-Aja et al. [25] and Oregui et al. [29]. Also, it is clear that when the toe stress increases, the rail pad's deformation decreases even under the same weight. On this effect, the toe load restricts the longitudinal and lateral deformation of the rail pad. The restriction rises as the toe load increases the compress. The rail pad will likely benefit from high preloads and become stiffer [30]. The information about toe load and its effect on restricting rail pad deformation is relevant in this study as it suggests that higher toe loads, resulting in increased compression, can lead to greater restriction and stiffness of the rail pad, which can influence its deformation behaviour under different frequencies and temperatures.

**Effect of frequency**

The results for dynamic stiffness under the effect of frequency are depicted in Figure 8. It has been observed that the stiffness of rail pads rises with frequency. This supports the findings provided by previous researchers [25]. Dynamic loads with a frequency of 20 Hz have the lowest deformation

compared to 2.5 Hz. In comparison between 2.5 Hz and 20 Hz, the different percentage of the deformation was 7.68%. The deformation is larger for a frequency of 2.5 Hz and it is notable that the deformation difference does not have much significance when the frequency is more than 5 Hz.

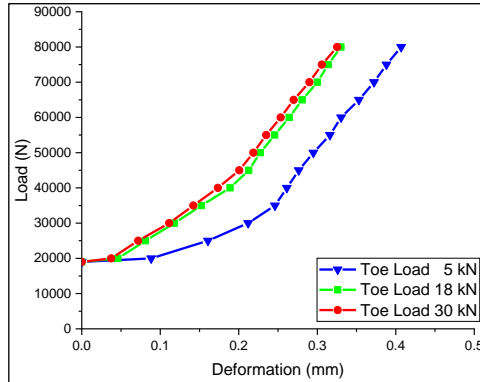


Figure 7: Toe load's impact on dynamic stiffness

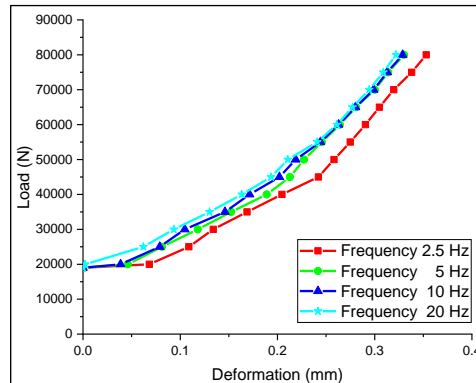


Figure 8. The effect of frequency load dependence on the dynamic stiffness

Figure 9 compares rail pad deformation for different frequencies and temperatures, providing insights from a mechanics and materials science perspective regarding the effect of heat. The reference case allows for comparison, revealing a significant disparity in deformation between high and low temperatures at the lowest frequency of 2.5 Hz. Conversely, at the highest frequency of 20 Hz, the difference in deformation is less pronounced. The average difference in deformation between high and low temperatures is measured at 16.87% for 2.5 Hz and 8.70% for 20 Hz. These results suggest

that, compared to lower frequencies, higher frequencies have a reduced impact on the dynamic stiffness of the TPE rail pad when subjected to temperature variations. These findings are consistent with Squicciarini et al.'s research [31], indicating that temperature decreases the rail pad's shear modulus while frequency increases it, thus influencing the dynamic stiffness of the elastomeric rail pad.

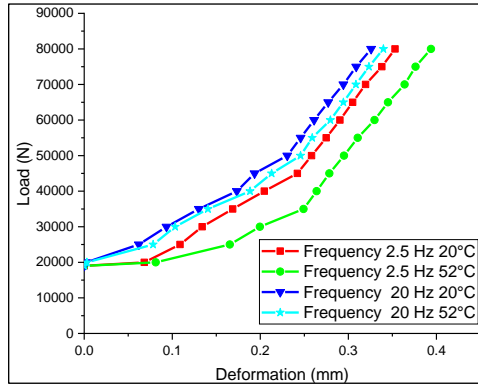


Figure 9: The dynamic stiffness of the rail pad at various temperatures and frequencies

## Conclusion

The predicted trends of dynamic stiffness using the FE method were found to be in good agreement with previous work, indicating the accuracy of the FE analysis method. The TPE rail pad displays high nonlinearity and variability with the loading condition. Temperature, toe load, and frequencies were the sensible factors that were investigated. The results of the simulation allow for the following inferences:

- i. The TPE rail pad's dynamic stiffness reduced as temperature decreased. It was normal for this kind of behaviour in polymeric materials. As temperature varied in the range of 0-52 °C, changes in stiffness were seen by fixing the other variables to reference standard values. The results demonstrated the great thermal sensitivity of the rail pad.
- ii. Toe loading correlated with dynamic stiffness. When the toe stress rises, the rail pad becomes firmer.
- iii. The displacement of the rail pad changes because of the rise in frequency in the range of 2.5 Hz and 20 Hz, growing into a sizeable distortion. This demonstrates how frequency influences the pads' dynamic stiffness. At low frequencies, the frequency impact becomes

significantly different. Typically, the rail pads get stiffer as the frequency rises.

In this simulation, comparing temperature and toe load, the frequency has a low influence on affecting the rail pad's dynamic stiffness. FE analysis, utilizing advanced simulation techniques and software like ANSYS, offers a cost-effective alternative to traditional physical testing methods in the railway industry. By creating virtual models of TPE rail pads and conducting simulations, engineers can accurately predict their behaviour under different operating conditions, including temperature variations. This eliminates the need for costly and time-consuming physical prototypes and extensive testing, resulting in substantial cost savings in material procurement, manufacturing, and experimental procedures. By integrating this degradation model into the FEM simulations, engineers can gain valuable insights into the potential degradation mechanisms of TPE rail pads, such as fatigue, creep, or material aging due to environmental factors. This enables them to forecast the performance degradation of rail pads and make informed decisions regarding maintenance schedules, replacement intervals, and overall system reliability. As a result, it might aid in the creation of decision support systems to improve maintenance and optimise track performance, hence reducing costs and prolonging the usable life of the infrastructure.

## **Contributions of Authors**

The authors confirm the equal contribution in each part of this work. All authors reviewed and approved the final version of this work.

## **Funding**

This work was supported by the “Fundamental Research Grant Scheme for Research Acculturation of Early Career Researchers (RACER/1/2019/TK03/UITM//2)”

## **Conflict of Interests**

All authors declare that they have no conflicts of interest

## **Acknowledgment**

The Ministry of Higher Education Malaysia financially supported this research through the Fundamental Research Grant Scheme for Research

Acculturation of Early Career Researchers (RACER/1/2019/TK03/UITM//2). The authors acknowledge the support received from the Ministry of Higher Education Malaysia. We also gratefully acknowledge Universiti Teknologi MARA for the preparation, execution, writing, and publication of this article.

## References

- [1] M. Sol-Sánchez, F. Moreno-Navarro, and M. C. Rubio-Gámez, “The use of elastic elements in railway tracks: A state of the art review”, *Construction and Building Materials*, vol. 75, pp. 293–305, 2015. doi: 10.1016/j.conbuildmat.2014.11.027.
- [2] M. Sol-Sánchez, F. Moreno-Navarro, and M. C. Rubio-Gámez, “The use of deconstructed tire rail pads in railroad tracks: Impact of pad thickness”, *Materials & Design*, vol. 58, pp. 198–203, 2014. doi: 10.1016/j.matdes.2014.01.062.
- [3] K. Knothe, M. Yu, and H. Ilias, “Measurement and Modelling of Resilient Rubber Rail-Pads,” *System Dynamics and Long-Term Behaviour of Railway Vehicles, Track and Subgrade*, vol. 6, pp. 265–274, 2003. doi: 10.1007/978-3-540-45476-2\_16.
- [4] . Ge, L. Ling, X. Yuan, and K. Wang, “Effect of distributed support of rail pad on vertical vehicle-track interactions”, *Construction and Building Materials*, vol. 262, p. 120607, 2020. doi: 10.1016/j.conbuildmat.2020.120607.
- [5] J. Chen and Y. Zhou, “Dynamic vertical displacement for ballastless track-subgrade system under high-speed train moving loads”, *Soil Dynamics and Earthquake Engineering*, vol. 129, no. November, pp. 1–10, 2020. doi: 10.1016/j.soildyn.2019.105911.
- [6] Z. Zeng, A. Ahmed Shuaibu, F. Liu, M. Ye, and W. Wang, “Experimental study on the vibration reduction characteristics of the ballasted track with rubber composite sleepers,” *Construction and Building Materials*, vol. 262, p. 120766, 2020. doi: 10.1016/j.conbuildmat.2020.120766.
- [7] S. Kaewunruen, A. Aikawa, and A. M. Remennikov, “Vibration Attenuation at Rail Joints through under Sleeper Pads”, *Procedia Engineering*, vol. 189, no. May, pp. 193–198, 2017. doi: 10.1016/j.proeng.2017.05.031.
- [8] N. Karpuschenko, D. Velichko, and A. Sevostyanov, “Effectiveness of Intermediate Rail Fastenings on the Railway Sections of Siberia”, *Transportation Research Procedia*, vol. 54, no. 2020, pp. 173–181, 2021. doi: 10.1016/j.trpro.2021.02.062.
- [9] C. Ngamkhanong, Q. Y. Ming, T. Li, and S. Kaewunruen, “Dynamic train-track interactions over railway track stiffness transition zones

- using baseplate fastening systems”, *Engineering Failure Analysis*, vol. 118, no. May, p. 104866, 2020. doi: 10.1016/j.engfailanal.2020.104866.
- [10] M. Sol-Sánchez, F. Moreno-Navarro, and M. C. Rubio-Gámez, “The use of deconstructed tires as elastic elements in railway tracks”, *Materials (Basel)*, vol. 7, no. 8, pp. 5903–5919, 2014.
- [11] J. Sadeghi, M. Seyedkazemi, and A. Khajehdezfuly, “Nonlinear simulation of vertical behavior of railway fastening system”, *Engineering Structures*, vol. 209, no. February, p. 110340, 2020. doi: 10.1016/j.engstruct.2020.110340.
- [12] A. Fenander, “Frequency dependent stiffness and damping of railpads”, *Proceedings of the Institution of Mechanical Engineers, Part F: Journal of Rail and Rapid Transit Part F J. Rail Rapid Transit*, vol. 211, no. 1, pp. 51–62, 1997. doi: 10.1243/0954409971530897.
- [13] K. Wei, Q. Yang, Y. Dou, F. Wang, and P. Wang, “Experimental investigation into temperature- and frequency-dependent dynamic properties of high-speed rail pads,” *Construction and Building Materials*, vol. 151, no. October 2018, pp. 848–858, 2017. doi: 10.1016/j.conbuildmat.2017.06.044.
- [14] K. Wei, P. Zhang, P. Wang, J. Xiao, and Z. Luo, “The influence of amplitude- and frequency-dependent stiffness of rail pads on the random vibration of a vehicle-track coupled system”, *Shock and Vibration*, vol. 2016, pp. 1-10, 2016. doi: 10.1155/2016/7674124.
- [15] S. Y. Zhu, C. B. Cai, Z. Luo, and Z. Q. Liao, “A frequency and amplitude dependent model of rail pads for the dynamic analysis of train-track interaction,” *Science China Technological Sciences*, vol. 58, no. 2, pp. 191–201, 2015. doi: 10.1007/s11431-014-5686-y.
- [16] K. Wei, F. Wang, P. Wang, Z. X. Liu, and P. Zhang, “Effect of temperature- and frequency-dependent dynamic properties of rail pads on high-speed vehicle–track coupled vibrations”, *Vehicle System Dynamics*, vol. 55, no. 3, pp. 351–370, 2017. doi: 10.1080/00423114.2016.1267371.
- [17] A. K. Mazlan, A. Malek, A. Wahab, M. A. Anuar, and A. K. Makhtar, “Nonlinear Static Stiffness of Rail Pads for Different Materials and Thicknesses using Finite Element Method”, *Journal of Mechanical Engineering*, vol. 11, no. 1, pp. 49–64, 2022.
- [18] S. G. Koroma, M. F. M. Hussein, and J. S. Owen, “The effects of railpad nonlinearity on the dynamic behaviour of railway tracks,” *Conference: Institute of Acoustics spring conference*, vol. 35, no. 1, pp. 176–183, 2013.
- [19] J. S. Bergstrom, *Mechanics of Solid Polymers*. Elsevier, 2015.
- [20] E. Kabo, J. C. O. Nielsen, and A. Ekberg, “Prediction of dynamic train-track interaction and subsequent material deterioration in the presence of insulated rail joints”, *Vehicle System Dynamic*, vol. 44, no. SUPPL. 1, pp. 718–729, 2006. doi: 10.1080/00423110600885715.

- [21] N. K. Mandal, “On the low cycle fatigue failure of insulated rail joints (IRJs)”, *Engineering Failure Analysis*, vol. 40, pp. 58–74, 2014.
- [22] M. I. H. Othman, A. M. A. Wahab, M. S. Hadi, and N. M. Noor, “Assessing the nonlinear static stiffness of rail pad using finite element method”, *Journal of Vibroengineering*, vol. 24, no. 5, pp. 921–935, 2022. doi: 10.21595/jve.2022.22293.
- [23] E. Harea, R. Stoček, and M. Machovský, “Study of friction and wear of thermoplastic vulcanizates: The correlation with abraded surfaces topology”, *Journal of Physics: Conference Series*, vol. 843, no. 1, pp. 1–9, 2017. doi: 10.1088/1742-6596/843/1/012070.
- [24] C. J. Ren *et al.*, “Anti-vibration slab mat to suppress train track vibrations”, *Journal of Engineering Science and Technology*, vol. 13, no. Special Issue, pp. 1–12, 2018.
- [25] J. A. Sainz-Aja, I. A. Carrascal, D. Ferreño, J. Pombo, J. A. Casado, and S. Diego, “Influence of the operational conditions on static and dynamic stiffness of rail pads”, *Mechanics of Materials*, vol. 148, no. June, pp. 1–19, 2020. doi: 10.1016/j.mechmat.2020.103505.
- [26] F. Nishino, S. Malla, and T. Sakurai, “Solution of finite-displacement small-strain elasticity problems by removal of rigid body displacements,” *Doboku Gakkai Ronbunshu*, vol. 2000, no. 661, pp. 11–26, Oct. 2000. doi: 10.2208/jscej.2000.661\_11.
- [27] K. Wei, Z. X. Liu, Y. C. Liang, and P. Wang, “An investigation into the effect of temperature-dependent stiffness of rail pads on vehicle-track coupled vibrations”, *Proceedings of the Institution of Mechanical Engineers Part F Journal of Rail and Rapid Transit*, vol. 231, no. 4, pp. 444–454, 2017. doi: 10.1177/0954409716631786.
- [28] R. A. Broadbent, D. J. Thompson, and C. J. C. Jones, “Evaluation of the effects of temperature on railpad properties, rail decay rates and noise radiation”, *16th Int. Congr. Sound Vib. 2009, ICSV 2009*, vol. 1, pp. 132–139, 2009.
- [29] M. Oregui, A. Núñez, R. Dollevoet, and Z. Li, “Sensitivity Analysis of Railpad Parameters on Vertical Railway Track Dynamics”, *Journal of Engineering Mechanics*, vol. 143, no. 5, p. 04017011, 2017. doi: 10.1061/(asce)em.1943-7889.0001207.
- [30] S. Kaewunruen and A. M. Remennikov, “An alternative rail pad tester for measuring dynamic properties of rail pads under large preloads”, *Experimental Mechanics*, vol. 48, no. 1, pp. 55–64, 2008. doi: 10.1007/s11340-007-9059-3.
- [31] G. Squicciarini, D. J. Thompson, M. G. R. Toward, and R. A. Cottrell, “The effect of temperature on railway rolling noise”, *Proceedings of the Institution of Mechanical Engineers, Part F: Journal of Rail and Rapid Transit*, vol. 230, no. 8, pp. 1777–1789, 2016. doi: 10.1177/0954409715614337.